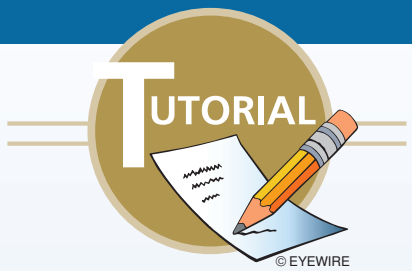

Robotics in the Small

Part I: Microrobotics

Approximately 400 years ago, the first optical microscopes were invented, and a previously unknown world became visible. One of the first uses of this new tool was in biology, and humans became aware of a variety of tiny yet complex microorganisms capable of locomotion and, apparently, sensing and limited intelligence [1]. This new tool was also used by craftsmen to extend their visual capabilities to make smaller and more complex timepieces and other precision devices. In a sense, the field of microrobotics was beginning, though it wasn't until the 1950s that integrated circuit manufacturing techniques started to develop, along with this the push toward making smaller and smaller electrical and, eventually, mechanical components. Coincidentally, it was also in this decade that physicists and biologists became actively interested in understanding how microorganisms such as bacteria and spermatozoa propel themselves. However, the robotics research community's interest in the microscale did not become sufficient for it to be considered a field in and of itself until the 1990s. In just over a decade, a tremendous amount of progress in microrobotics has been made, but as will become apparent in this article, we are only just beginning.

As a working definition, we consider the field of microrobotics to include the robotic manipulation of objects with characteristic dimensions in the millimeter to micrometer range (micromanipulation) as well as the design and fabrication of robotic agents in a similar size range (microrobots). Applications of micromanipulation include, for example, manipulation of biological cells and assembly of microsized parts. These tasks require novel tools and sensors that operate at the microscale. However, as we will see, the scaling of physical effects makes even the simplest manipulation tasks challenging. Microrobots have been proposed for numerous applications ranging from in vivo biomedical therapy to military reconnaissance. Due to the scaling of physical effects, microrobots operate in a world that seems foreign to our intuition. In addition, traditional fabrication and power-supply methods become unfeasible at the microscale. Consequently, novel technologies must be considered in the design of microrobots. As dimensions go below the micrometer range, we enter the realm of nanorobotics, which is the focus of Part II of this tutorial.

Conversations on microrobots, especially when applied to biomedical applications, inevitably turn to the film *Fantastic Voyage* (Figure 1). In *Fantastic Voyage* a team of scientists and their submarine are miniaturized using a top-secret technology, enabling them to navigate through the human blood stream to save the life of a dying man. This is an imaginative vision of noninvasive surgery, but the problem is that even if this amazing shrinking technology existed, the miniature submarine and its crew would be totally ineffective. The submarine's propellers would not function at that scale. The crew would not be able to walk around inside the submarine because of the adhesive forces between their feet and the floor. Even if the crew could make it out of the submarine, the tiny SCUBA divers could kick their legs all day and go nowhere.

This example illustrates the key to understanding microrobotics. Microrobotics is not simply about making traditional robots smaller. To work in microrobotics, we must let go of some of the intuition that we have built as engineers, and we must build new intuition. Robotics is often described as an interdisciplinary topic, and microrobotics takes this to another level; we must have an understanding of many additional topics in physics, material science, and biology. To understand microrobotics, we must begin with a discussion of how physical effects manifest at the microscale. We must also be familiar with the basic methods of microfabricating tiny components. With that background knowledge, we can explore the two major topics in microrobotics: micromanipulation and the design of microrobots.

BY JAKE J. ABBOTT, ZOLTÁN NAGY, FELIX BEYELER, AND BRADLEY J. NELSON

1070-9932/07/$25.00©2007 IEEE

Scaling of Physical Effects

The microscopic world is governed by the same physical laws as the macroscopic world but the relative importance of the physical laws changes. When we talk about scaling, we refer to some characteristic length L of the device of interest. We then assume that all dimensions scale linearly proportional to L. Thus, as we scale a device, its volume scales as $\sim L^3$, while its surface area scales as $\sim L^2$. Volume is associated with inertia, weight, heat capacity, and body forces. Surface area is associated with friction, heat transfer, and surface forces. It is the balance between volume and surface effects that leads to many of the scaling issues important in microrobotics. There are a number of works that deal with the topic of scaling [2]–[6], and a thorough overview is beyond the scope of this article. We will, however, discuss a few of the scaling issues that are particularly important in microrobotics: attractive and repulsive forces and fluid mechanics.

Attractive and Repulsive Forces

Electrostatic forces are widely considered to scale well to the microscale. Let us consider the electrostatic force between two parallel plates and examine how that force is affected by scaling. Let A denote the surface area of the plates, and let x be the separation distance. The capacitance is given by

$$C = \varepsilon \frac{A}{x,} \tag{1}$$

where ε is the permittivity of the dielectric material separating the plates. The capacitance relates a voltage U that is applied to the plates to the charge Q that is accumulated on each plate: $Q = CU$. The electrostatic co-energy stored in the capacitor can be expressed by

$$W = \frac{1}{2} CU^2, \tag{2}$$

and the attractive force between the plates is computed as $F = -dW/dx$.

We will consider two situations: holding voltage constant and holding charge constant. In the case of constant voltage:

$$F_{\mathrm{U}} = \frac{\varepsilon A U^2}{2x^2}. \tag{3}$$

In the case of constant charge:

$$F_{\mathrm{Q}} = \frac{Q^2}{2\varepsilon A}. \tag{4}$$

Note that (1)–(4) assume x is small relative to the dimensions of the plates. The scaling behavior of the force laws depends on the scaled quantities. For example, consider scaling only the dimensions of the plate as $\sim L$. The area A is scaled as $\sim L^2$, thus, F_{U} scales as $\sim L^2$ and F_{Q} scales as $\sim L^{-2}$. If we scale the gap distance x as well, F_{U} remains constant whereas F_{Q} still scales as $\sim L^{-2}$.

The scaling of magnetic effects has been discussed with seemingly conflicting conclusions, ranging from being very poor [3] to one of the most promising actuation methods at the microscale [6]. Both standpoints can be correct, depending on the scaled and examined quantities. Consider for example the force between two identical magnets with magnetization M and volume v, aligned along their dipole axes, and separated by a distance x. The field created by one magnet along its axis is expressed using the point dipole model as

$$H(x) = \frac{Mv}{2\pi x^3.} \tag{5}$$

The magnitude of the attractive/repulsive force on the other magnet is then given by

$$F_{\mathrm{m}} = \mu_0 M v \left| \frac{\partial H}{\partial x} \right| = \frac{3\mu_0 M^2 v^2}{2\pi x^4,} \tag{6}$$

where μ_0 is the permeability of free space. Note that the magnetization M remains constant for scaling as it is an intrinsic physical property of the magnets.

If we scale the magnets down as $\sim L$ but hold the distance between the magnets constant, the force will be scaled as $\sim L^6$, resulting in a very poor scaling. However, if we also scale the distance between magnets as $\sim L$, the force is scaled as $\sim L^2$, which is significantly better. Finally, if instead of force, we consider the force-to-volume ratio F_{m}/v in the second case, we find that the force is scaled as $\sim L^{-1}$ and thus increased. Other magnetic interactions such as magnet-iron, magnet-coil, coil-iron, and coil-coil, as well as induction effects can be analyzed in an analogous manner [6].

The scaling of adhesion forces is of particular interest because they are always present, and their importance relative to other forces increases as size decreases. Consider for example the intermolecular van der Waals force between a sphere with radius r and an infinite halfspace:

Figure 1. *In* Fantastic Voyage, *a submarine and its crew are miniaturized to save the life of a dying man from the inside. Image ©20th Century Fox.*

$$F_{\text{vdW}} = \frac{H r}{8\pi x^2}, \tag{7}$$

where x is the separation distance and H is the material-dependent Hamaker constant that is typically on the order of 10^{-21}–10^{-20} J. Scaling only the radius of the sphere as $\sim L$ results in $F_{\text{vdW}} \sim L$. If, in addition, x is scaled as $\sim L$, the force will scale as $\sim L^{-1}$, and thus its importance increases at the microscale. In the case of sufficiently high humidity of the surrounding environment, a liquid water film can form between the sphere and the halfspace, and the resulting surface tension force has to be considered as well. It can be approximated as

$$F_{\text{tens}} = 2\pi\gamma r, \tag{8}$$

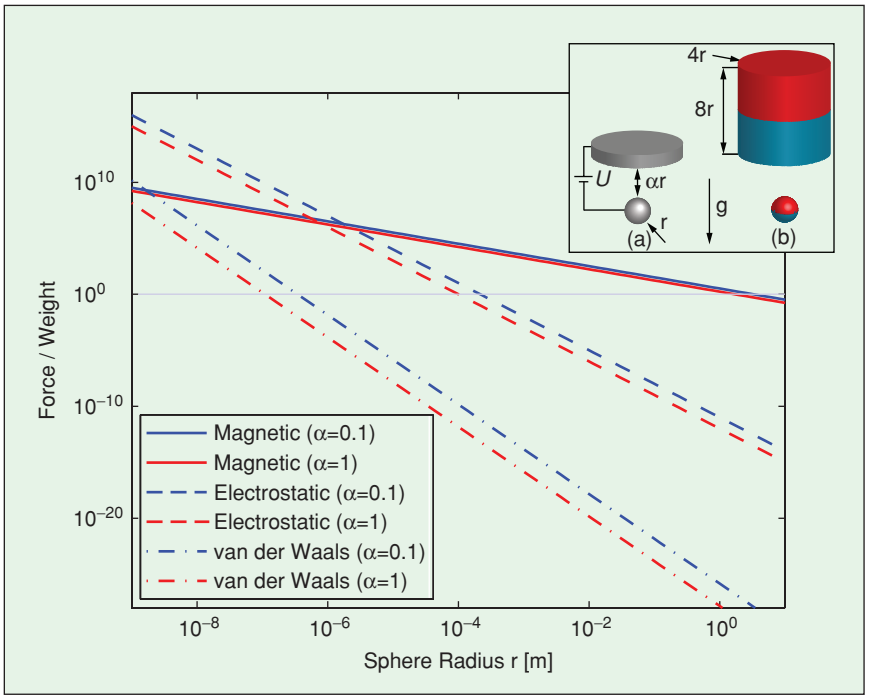

Figure 2. *Results of scaling of attractive forces. For the calculations, typical values are used ($\rho = 6.72 \times 10^3$ kg/m^3, $U = 100$ V, $M = 1.1 \times 10^6$ A/m). For $r < 1$ m, the magnetic force is sufficient to lift the sphere. Below $r = 10^{-4}$ m, the electrostatic force dominates over gravity, and for $r < 10^{-7}$ m, the van der Waals force is higher than the weight of the sphere.*

where γ is the material-dependent surface tension (in N/m). Observe that $r \sim L$, and thus $F_{\text{tens}} \sim L$. Note that surface tension is an aggregate manifestation of van der Waals forces.

Let us illustrate the effect of scaling using a simple example. Imagine that the task is to lift (against gravity) a sphere using a tool with electrostatic or magnetic forces. In the former case, let both bodies be made of conducting material and have a potential difference U, while in the latter, let both be permanent magnets and aligned along their magnetization (see Figure 2).

For the electrostatic interaction, we assume the tool to behave as an infinite halfspace to simplify the calculations. The magnetic force is determined, assuming a cylindrical tool with radius $4r$ and a height $8r$, where r is the radius of the sphere. In both cases, the sphere-tool distance is αr. This allows us to examine scaling effects as we vary only r. For the calculations, typical values are used for free parameters, and the results are shown in Figure 2. As seen in the figure, gravity is governing the interaction for $r > 1$ m, whereas magnetic force dominates over gravity for $r < 1$ m followed by the electrostatic force for lower r. For $r < 10^{-4}$ m, the electrostatic force is sufficient to lift the sphere, and for $r < 10^{-6}$ m the electrostatic force dominates the magnetic force. Increasing α, the dimensionless distance between the sphere and the tool, basically shifts these limits to lower values.

In addition to the magnetic and electrostatic forces, the van der Waals force is also shown in Figure 2. Note that its contribution is already more important than gravity for $r < 10^{-7}$ m. As observed from the trends in Figure 2, its importance increases as we continue to scale down.

Fluid Mechanics

The Navier-Stokes equations, when combined with appropriate boundary conditions, completely define a fluid's velocity in space and time (assuming that there is no phase transition). For an incompressible fluid with constant viscosity, they are given by the vector equation

$$\rho \frac{d\mathbf{V}}{dt} = -\nabla p + \eta \nabla^2 \mathbf{V}, \tag{9}$$

where $\mathbf{V}$ is the velocity vector field, p is the hydrodynamic pressure scalar field, and ρ and η are the fluid's constant density and viscosity, respectively. If we substitute the following nondimensional variables into (9):

$$\tilde{x} = \frac{x}{L}, \quad \tilde{\mathbf{V}} = \frac{\mathbf{V}}{V_s}, \quad \tilde{t} = \frac{tV_s}{L}, \quad \tilde{p} = \frac{pL}{\eta V_s}, \tag{10}$$

where x is a Cartesian coordinate variable, V_s is the magnitude of the free-stream velocity, and L is a characteristic length of the object of interest, we arrive at the nondimensional Navier-Stokes equations

$$\left(\frac{\rho V_s L}{\eta}\right) \frac{d\tilde{\mathbf{V}}}{d\tilde{t}} = -\tilde{\nabla}\tilde{p} + \tilde{\nabla}^2 \tilde{\mathbf{V}}. \tag{11}$$

From this equation, we discover the Reynolds number, which is the dimensionless quantity that embodies the interaction between a fluid's inertia and viscosity as it flows around an object:

$$Re = \frac{\rho V_s L}{\eta}. \tag{12}$$

Most engineers have little intuition about low-Re regimes, which is typically defined by approximately $Re < 10$. Our intuition about fluid behavior is associated with significantly higher Re, where we must deal with transitions from laminar to turbulent flow. At high Re, we are familiar with concepts such as streamlining to reduce drag, and most engineers have some intuition about whether or not a shape is hydrodynamic. At low Re, we are in a world that is either very viscous, very slow, or most importantly for our present discussion, very small. We no longer see a transition to turbulence, even behind bluff bodies. We find that at low-Re terms in the fluid become negligible, and a simple equation governs the flow:

$$\tilde{\nabla}\tilde{p} \approx \tilde{\nabla}^2 \tilde{V}. \tag{13}$$

Note that time no longer appears in (13). Consequently, the flow pattern does not change appreciably, whether it is slow or fast, and the flow is reversible. Low-Re flow around a body is referred to as creeping flow or Stokes' flow.

There is one particularly useful low-Re result worth mentioning. The viscous drag force on a sphere with diameter d in an infinite extent of fluid can be calculated as a linear function of the sphere's velocity through the fluid:

$$F_{\text{drag}} = 3\pi\eta d V_s. \tag{14}$$

This is known as Stokes' law and is valid for at least $Re < 1$. Because the shape of the body becomes less important as we reduce Re, Stokes' law is a good predictor of drag force on a variety of shapes.

Microfabrication

Microfabrication is the term for fabricating structures on a micrometer scale [7]. Unlike traditional serial fabrication processes, such as milling, lathing, and assembly with nuts and bolts, microfabrication is based on manufacturing many identical structures in parallel, also known as batch fabrication (see Figure 3). This parallelism enables the production of a large number of devices at a relatively low price. Microfabrication technologies are based on fabrication processes that have been developed for the semiconductor industry. Traditional microfabrication methods are limited to planar two-dimensional (2-D) patterns with lateral dimensions ranging from ones to thousands of micrometers and thicknesses in the nanometer to micrometer range. With the advent of microelectromechanical systems (MEMS), new processes and three-dimensional (3-D) fabrication methods are continually being developed and improved. Because material usage scales with volume, material costs for microfabricated devices are typically much lower than for macro devices. Processing, testing, and packaging costs are more important.

Devices are normally fabricated on silicon wafers, but other materials such as glass or polymer substrates are also used. Two strategies for building devices exist: surface and bulk microfabrication. Surface microfabrication is the deposition and patterning of thin film layers on the surface of the substrate. Bulk microfabrication patterns and etches cavities into the substrate to form parts of the device. With the growth of MEMS, new processes and materials are continually being developed and adopted to increase the scope of microfabrication, and traditional boundaries are becoming blurred.

Structures on the wafer are created by a sequence of fabrication steps performed in a cleanroom facility. The most important process building blocks are material deposition, pattern transfer, and etching. Deposition processes are used to create thin films of a material on the wafer. Commonly used processes are physical or chemical vapor deposition, electroplating, and spinning. Pattern transfer is typically accomplished with photolithography. Common photolithography uses metallic patterns on glass plates to shield or expose photosensitive layers (photoresist) to light. These layers can then be selectively removed depending on their exposure. Etching processes are typically divided between wet and dry processes. Wet etching means etching material in a chemical solution. Dry etching is performed by a vapor phase etchant or by reactive ions. By repeating material deposition, photolithography, and etching steps, complex microsystems can be built. Figure 4 illustrates a simple microfabrication process to create multiple copies of aluminum electrodes on a wafer, including metal deposition, photolithography and metal etching.

Micromanipulation

Micromanipulation is the robotic manipulation of objects with characteristic dimensions in the millimeter to micrometer range. Single-axis and multi-axis micromanipulators are commercially available with a travel range of a few millimeters or centimeters and with a resolution typically better than 1 μm. Stages are typically driven by dc motors, stepper motors, or piezo drives. Some micromanipulators provide

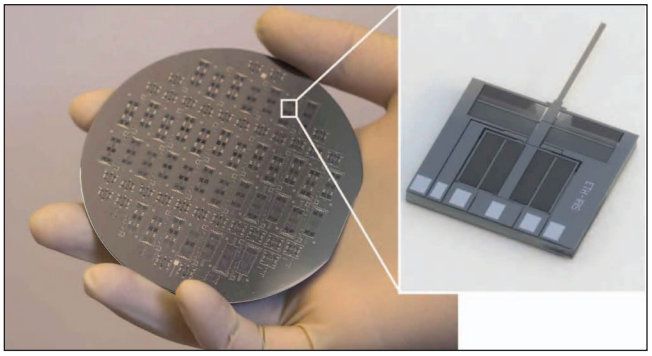

Figure 3. *A silicon wafer that includes many micro force sensors.*

encoders for accurate position feedback. In most cases, micromanipulation tasks are observed by an optical microscope.

Manipulation of microscale parts requires the use of miniaturized tools with end-effectors on the size-scale of the manipulated objects. Most micromanipulation is done with microrobotic tools such as probes, micropipettes, or microgrippers. Microgrippers that have been developed in recent years are actuated using a variety of methods, such as electrostatics, thermal expansion, piezoelectrics, magnetism, or shape memory alloys [8]. Figure 5 shows a silicon microgripper mounted on a commercially available three-axis micromanipulator. The gripper is only a few millimeters in size and is capable of picking up objects ranging 5–200 μm in size [9].

In micromanipulation, even the simple task of picking up a part and placing it in new location becomes challenging. The forces arising during micromanipulation have to be well controlled in order to successfully manipulate microobjects. These forces are dominated by surface tension forces, electrostatic forces, and van der Waals forces, normally ranging from tens of nano-Newtons to several micro-Newtons [4], [10]. Steps can be taken to mitigate undesirable consequences of these forces [10]. Some of the potential part-handling methods that make use of these forces are illustrated in Figure 6.

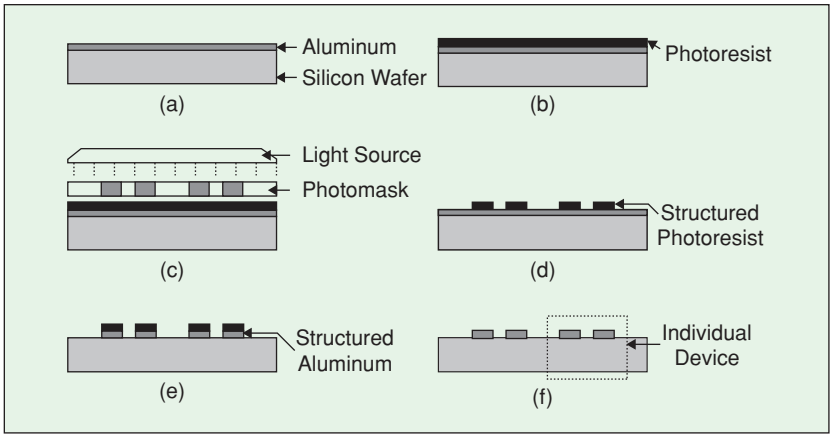

Figure 4. *Fabrication of aluminum electrodes on a wafer. (a) Aluminum is deposited on a silicon wafer by physical vapor deposition. (b) A thin layer of photoresist is deposited on the wafer, and (c) exposed to UV light through the transparent areas on the photomask. (d) The wafer is immersed into developer, causing the photoresist to selectively dissolve depending on its exposure to UV light. (e) The wafer is immersed into acid, etching the aluminum where it is not protected by photoresist. (f) The photoresist is stripped by a solvent.*

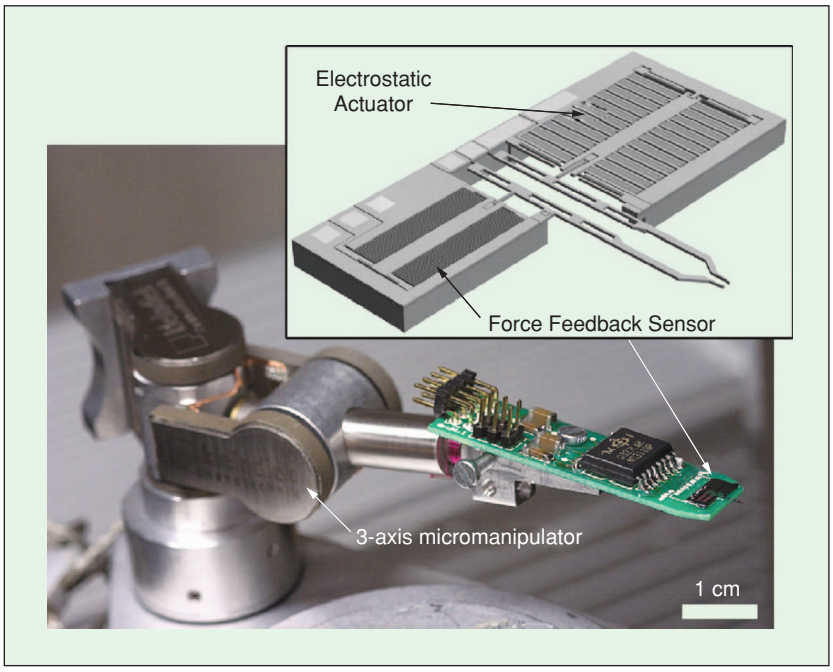

Figure 5. *MEMS force-feedback microgripper mounted on a Kleindiek MM3A three-axis piezo-driven micromanipulator.*

In order to measure and characterize forces during manipulation, several MEMS force sensors have been developed. One common transduction technique is measurement of force as a change in resistance using strain gauges or piezoresistive elements [11]. Another common technique is measuring a change in capacitance between two electrodes, where the gap is a function of the applied force [12].

Manipulating Biological Cells

Since most animal cells (including human) range in size between 1 and 100 μm, microrobotic tools are required to manipulate single cells. Cell manipulation is one of the most important applications for microrobotics. One typical task in genetic engineering and transgenics is the injection of substances into a cell. The cell is held in place by a vacuum holding pipette, while an extremely fine micropipette penetrates the cell membrane, and sometimes the nuclear envelope, to release its contents. The microinjection is normally performed under a microscope and the pipettes are positioned by micromanipulators (see Figure 7).

We can go beyond basic microinjection by using other microrobotic tools. For example, microgrippers can be used as an alternative to holding pipettes for the positioning of cells [13]. In [9], cells are first aligned by ultrasonic pressure fields inside a microfluidic channel before being manipulated by microgrippers. We can also use the tools of microrobotics to study the mechanical properties of the cell itself. For instance, micro force sensors are used to characterize the hardening of cell membranes after fertilization [14], as well as to calibrate vision-based force sensing through the observation of cell-membrane deformation [15].

Microassembly

Another important application of micromanipulation is microassembly [16], [17]. Microassembly allows us to break free of the confines of planar microfabrication processes and create complicated 3-D structures. Microassembly also facilitates the development of hybrid-MEMS, which is the fabrication of devices that incorporate incompatible MEMS technologies. Figure 8 shows the microassembly of two components of a soft-magnetic microrobot (discussed later in this article).

In addition to the problems with parts handling previously discussed, another important problem in microassembly is joining parts. At the microscale, fasteners become infeasible, and adhesives (glue) become more practical, although surface tension makes their use challenging as well. UV-cured glues are useful, since the curing process is delayed, allowing time for proper assembly. Another method of joining parts is to fabricate interlocking components into the parts, such that they snap together. This creates a more complicated microfabrication process, but can simplify microassembly.

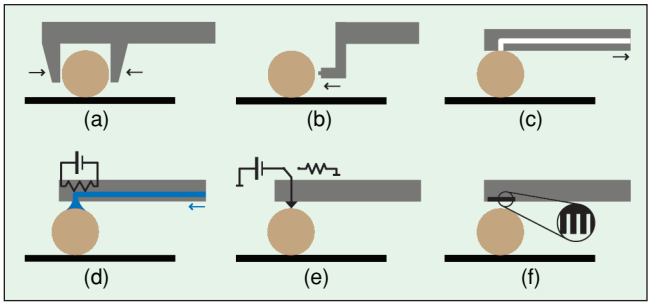

Figure 6. *Strategies for gripping microparts (based on [4]). (a) Using traditional gripping methods, the part is released when gravity pulls it away from the gripper. (b) Impulsive forces can can be used to push the part in a desired direction. (c) A vacuum becomes efficient as scale reduces, since the weight of the part decreases relative to the surface area. (d) Surface tension due to fluids (water) can be used to hold parts. The water can be vaporized to release the part. The water can also be frozen to form a rigid connection. (e) Electrostatic charges can be used to grip parts. Grounding the charge can be used to release the part. (f) Changes in surface roughness lead to changes in van der Waals forces, since surface molecules are farther apart, on average, with rough surfaces than with smooth. A part can be gripped with a smooth portion of the gripper, and then released by rolling/sliding it to a rough portion.*

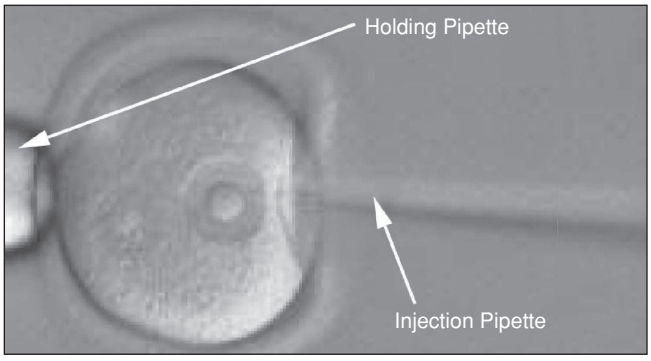

Figure 7. *Penetration of a mouse egg cell membrane.*

Microassembly is not as deterministic as traditional robotic assembly. It is difficult to automate because the parts might not be exactly where expected, or the gripping/releasing procedure did not work exactly as planned. Consequently, a great deal of sensor feedback is needed during microassembly, specifically visual feedback. This is difficult, as vision systems working at the microscale have limitation when compared to their macroscale counterparts. Pin-hole camera models lose validity with microscopes. The depth of field can be small, so only small portions of the workspace might be in focus at a given instant. It may not be possible to have stereo cameras.

Microassembly represents a bottleneck in the construction of microscale devices. As described previously, microscale parts are batch fabricated in large quantities, yet microassembly is typically a serial process. Consequently, it is very desirable to either develop parallel microassembly processes or automate serial microassembly. This is a challenging problem, and will essentially require solutions to each of the problems discussed above.

Microrobots

We are now equipped with an understanding of scaling effects and fabrication techniques for microscale devices, and we are

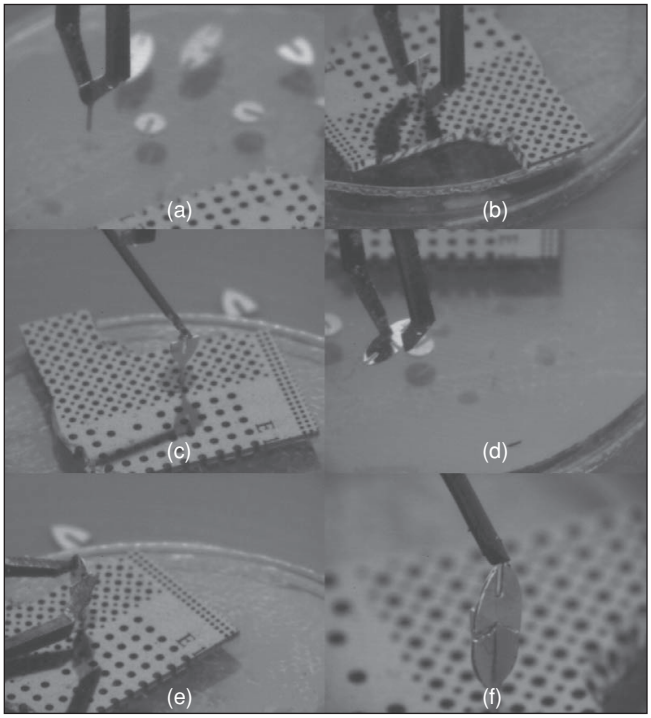

Figure 8. *Sequence of a manual assembly process where component B of the microrobot is inserted in component A. (a) Component A is grasped and (b) inserted into a hole of the workbench. (c) UV-activated glue is applied. (d) Component B is picked up and (e) inserted into Component A. (f) The assembly of the two components is complete. The largest component in this microrobot (component B) is 940 μm long, 400 μm wide, and 50 μm thick.*

ready to develop microrobots: robotic agents in the millimeter to micrometer range. In this section, we look to nature as a source of inspiration for our microrobot designs, and we discuss the challenging topic of power supply. Finally, we examine various microrobot designs that have been conceived to date.

Inspired by Nature

Nature has a great deal to teach us about microrobot design. Microorganisms are proof that systems functioning at the microscale can exhibit amazing levels of functionality. Microorganisms are able to swim at low Re using a variety of techniques that differ from our intuition about swimming at higher Re [2], [18]. A consequence of the lack of time in (13) is that any reciprocal motion (i.e., any body motion that simply goes back and forth between two configurations) will result in no net movement. Below about $Re = 10$, nature does not use life in either flying or swimming (no wings or propellers), and instead uses drag. To visualize swimming or flying using drag, imagine paddling a canoe. The paddle has a broad side that is held normal to the flow during the power stroke and held parallel to the flow (or removed from the water entirely) during the recovery stroke. At low Re, an almost ideal paddle is a cylinder with the long axis held perpendicular to the flow during the power stroke and parallel to the flow during the recovery stroke. This is the paddling method of cilia, which is used by microorganisms such as Paramecium [Figure 9(a)].

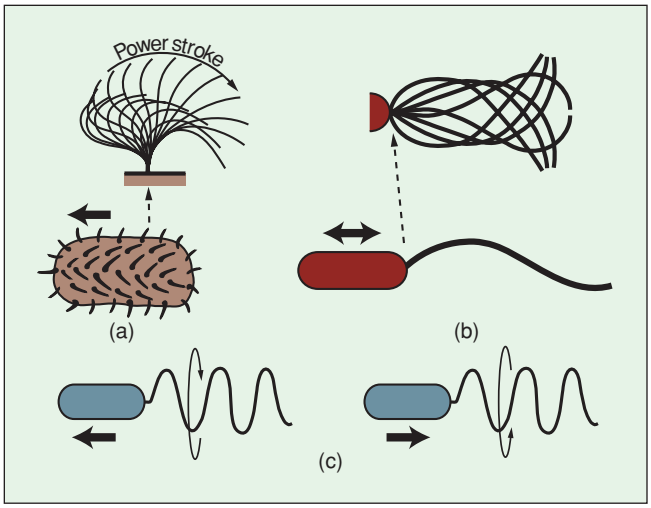

Figure 9. *Locomotion of microorganisms. (a) Cilia move across the flow during the power stroke, and fold near the body during the recovery stroke. (b) Eukaryotic flagella create patterns such as propagating waves or circular translating movements. (c) Molecular motors spin bacterial flagella, which act like corkscrews.*

Figure 10. *Microscope photo of a thrips, a bristle-wing insect with a body length that can be less than 1-mm long. Image © Peter S. Gillespie, NSW DPI, Australia.*

Another propulsion mechanism of microorganisms is eukaryotic flagella, which are active organells that deform to create paddling motions [Figure 9(b)]. The eukaryotic flagella can create propagating waves or circular translating movements. Eukaryotic flagella do not have to act as a tail, microorganisms can also swim with their flagellum in the front. Bacterial (prokaryotic) flagella work differently by using a molecular motor to turn the base of the flagella, which acts like a corkscrew [Figure 9(c)]. Some bacteria have multiple flagella that bundle during swimming. The entire length of a bacterial flagellum is used for propulsion at any given time, making them more efficient than the methods previously discussed. Even so, bacterial flagella are fairly inefficient; a bacteria moves forward only about 7% as far as it would if its flagellum were a rigid corkscrew moving through a cork. However, the inefficiency of microorganisms is not a problem because their source of energy (food) is so plentiful.

Some very small swimming and flying organisms have bristles-bearing appendages (bristles are sometimes referred to as hairs or fringes). The bristles can act as rakes to gather food by filtering water, and as the Reynolds number decreases they can act as paddles that can be folded together to reduce drag during the recovery stroke. It is the Reynolds number that determines if a bristle-bearing appendage will act as a rake or a paddle. Some small crustaceans swim and gather food with bristles. Bristles also act as wings with no continuous membrane for the very smallest flying insects, such as the thrips shown in Figure 10.

Insects and spiders demonstrate the ability to walk on walls and ceilings. We can learn about walking with adhesion by studying the feet of these small creatures. For example, jumping spiders use dry adhesion. The special structure of a jumping spider's foot provides a great deal of exposed surface, leading to large van der Waals forces (Figure 11(a) and [19]). Ants, on the other hand, use wet adhesion to stick to surfaces. The ants secrete an adhesive fluid, which creates surface tension under an adhesive pad (arolium) on the ant's foot (Figure11(b) and [20]). By controlling contact area, ants walk and run on adhesive pads that individually possess the ability to hold more than the entire body weight of the ant through

surface tension. Both spiders and ants have adapted passive mechanisms to mitigate the effects of adhesion when they are unwanted (i.e., during walking and jumping).

We can learn more from nature than just mechanical design. Ongoing research aims at the complete reverse engineering of fruit-fly (Drosophila) flight (Figure 12). A MEMS force sensor (the same shown in Figure 3) is used to measure the lift force generated by the wings during flight [21] while high-speed computer-vision techniques are used to capture the wing kinematics. These novel sensing techniques measure the system outputs, and to provide a system input, a virtual environment for the fruit fly creates visual patterns that simulate various types of movement (e.g., forward or upward). With the ability to provide controlled system inputs and accurately measure system outputs, a thorough understanding of how Drosophila fly is just over the horizon. This line of research can be applied toward the design of flying microrobots like those discussed later in this article.

What About Power?

Power supply for microrobots is a challenging and ongoing research topic, and it is probably the single biggest obstacle to achieving functional microrobots. The power systems we will consider range from being completely on-board to being completely supplied by the environment.

On-board power supplies are basically miniaturizations of existing macro scaled generators (e.g., batteries). Batteries offer an inexpensive power source if the size is acceptable. Note that the term microbattery is employed by battery producers to designate the coin cell type batteries used, for example, in watches. These batteries are not microsized at all but rather have a volume of around 0.1–0.2 cm^3. Rechargeable thin film batteries are a type of battery possibly suitable for microrobotic applications. The difference to traditional batteries is that thin film batteries are fabricated using semiconductor technologies like those previously discussed. Since these

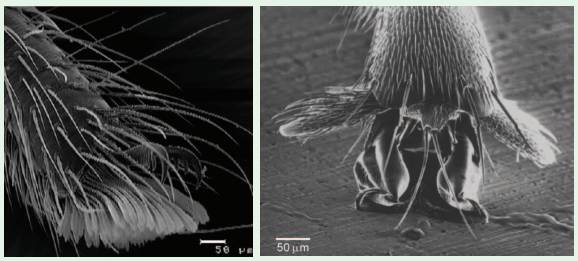

Figure 11. *(a) SEM image of the foot of a jumping spider* E. arcuata. *Image courtesy Andrew Martin, University of Applied Sciences, Bremen, Germany. (b) SEM image of the foot of an Asian weaver ant* O. smaragdina. *The two claws and the adhesive pad in surface contact are visible as well as deposited droplets of adhesive secretion. Image courtesy Walter Federle, University of Cambridge, U.K.*

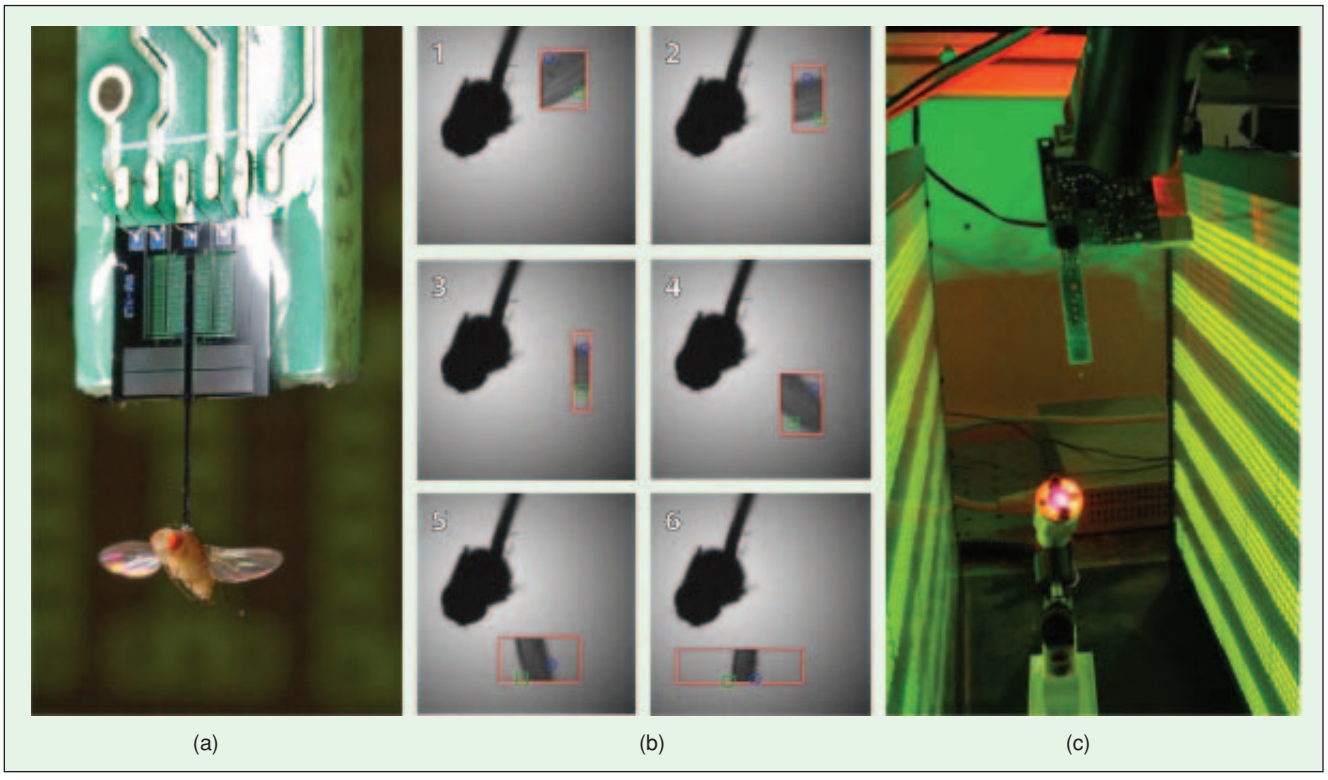

Figure 12. *Reverse engineering Drosophila flight. (a) A MEMS force sensor accurately measures lift force. (b) High-speed computer-vision techniques allow real-time measurement of wing kinematics. Kalman filtering is used to estimate the wing position, and a camera with a dynamic region of interest only transfers pixels around the current wing position. (c) A virtual environment with a fast refresh rate creates controlled visual inputs to the insect's flight control system.*

are planar processes, almost arbitrarily shaped batteries are possible with thicknesses below 50 μm. This allows product design with optimal use of available space.

MEMS-based power generators (Power MEMS) are interesting, as they promise higher energy densities than traditional generators and batteries [22]. Several research groups have presented transducers to convert various types of energy into electrical energy. Many make use of on-board chemical fuels. There are also designs that harvest thermal energy from the environment as well as designs that scavenge mechanical energy (through the form of vibrations) from the environment. Solar cells can also be integrated onto a microrobot that convert the radiation of the sun, or other sources, into useful energy. This technology is also promising as it scales with the surface rather than volume (as with batteries, for example).

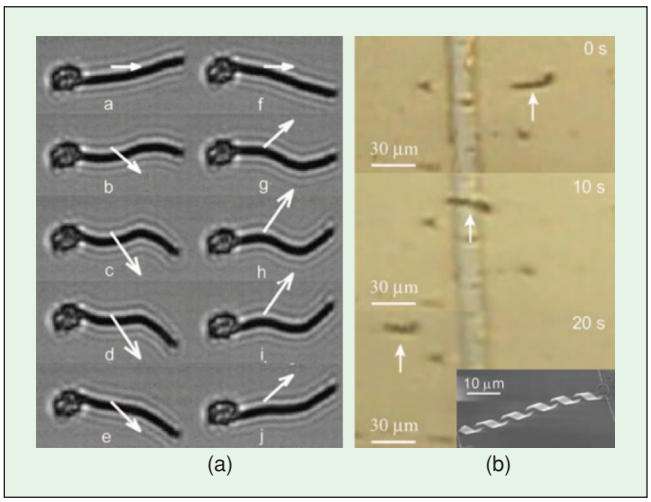

Figure 13. *(a) An artificial eukaryotic flagellum attached to a red blood cell. Arrows indicate the direction of the applied magnetic field. The swimmer moves from left to right. Image courtesy Rémi Dreyfus, École Supérieure de Physique et de Chimie Industrielles, France. (b) An artificial bacterial flagellum constructed from a nanocoil attached to a ferromagnetic disk. A swimmer moves from right to left due to a rotating magnetic field. In both cases shown, the flagella are leading the bodies, and do not act as tails.*

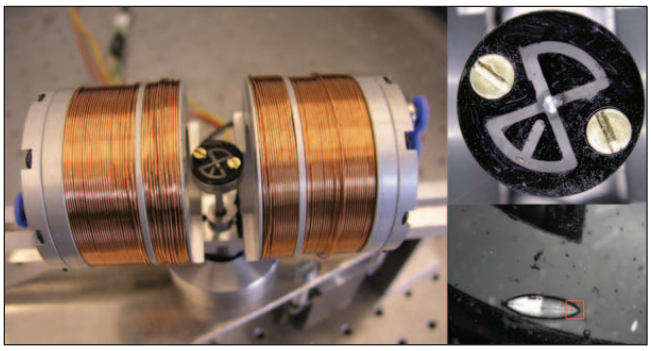

Figure 14. *A 900 μm $\times$ 400 μm assembled-MEMS microrobot navigating a fluid-filled maze. A motorized magnetic coil system provides computer-controlled field magnitude, orientation, and gradient.*

In contrast to carrying or producing energy on-board, a microrobot can be placed into an external field (e.g., a magnetic field). Using inductive coupling, the energy of an alternating magnetic field is converted into electrical power. A challenge here is the design of the receiver coil, since microfabricated coils are constrained by planar microfabrication processes. Besides converting an external magnetic field into electricity, the field can be used to actuate a microrobot directly. By fabricating parts of the microrobot out of magnetic material, torques and forces can be applied to the untethered microrobot. Note that electric fields could possibly be used as well. However, consider that it is comparatively simple to generate magnetic fields over large distances, whereas no equivalent generation methods exist for electric fields.

Finally, a very desirable option is for the microrobot to harvest chemical energy directly from the biochemical environment in which it is operating. We discussed previously how microorganisms are able to swim using very inefficient techniques because their energy supply through food is so large. Consider, for example, a microrobot inside the human body that navigates through the cardiovascular system. It could use the glucose in the blood to power simple circuits using a biofuel cell, such as presented in [23].

Conceived by Engineers

For the remainder of this article we discuss actual microrobot design concepts. These designs range in size and utilize an array of locomotion strategies, including swimming, crawling, flying, and simply moving passively with the environment.

The simplest type of microrobot is passive, containing no controlled form of locomotion. It simply moves as its environment dictates. Passive microrobots could move with the current of a fluid, for example in the bloodstream, or could move through the gastrointestinal (GI) tract due to peristalsis [24]. As we design robots at true micro scales, passive microrobots may be some of the most feasible, since they require no actuators (at least not for locomotion), and consequently have minimal power requirements.

Just as most microorganisms live in fluid environments, swimming has been the focus of a great deal of microrobot research. Swimming typically refers to movement in a liquid through body deformations, but we use the term more loosely here to refer to any locomotion through a liquid environment. The idea of mimicking flagellar swimming in microrobots has been discussed for some time [25], and recently flagellar swimming has actually been demonstrated at the microscale. In [26], an artificial eukaryotic flagellum is attached to a red blood cell [Figure 13(a)]. By controlling the direction of an applied magnetic field, a movement like a propagating wave is generated in the flagellum, causing the modified red blood cell to swim. In [27], a nanocoil is used as an artificial bacterial flagellum [Figure 13(b)]. The nanocoil is attached to a ferromagnetic disk, and a rotating magnetic field applies torque to the disk, which causes the microrobot to swim. It is also possible to mimic the corkscrew swimming strategy of bacterial flagella in ways that are not exhibited in

nature. For instance, if a microrobot takes on the shape of a screw [28], the swimming methodology is the same as before, without the need for a dedicated flagellum that increases the overall size of the microrobot.

We have demonstrated how external magnetic fields can be used to mimic flagellar swimming, which is proven to be effective at the microscale. However, natural selection may lead to only locally optimal designs, and in addition, as engineers we can apply methods of propulsion that would be impossible for autonomous microorganisms. For instance, we can wirelessly pull on the microrobot. Simple models indicate that this may be a desirable strategy over flagellar swimming [2]. In Figure 14 [29], a soft-magnetic assembled-MEMS microrobot (the microrobot being assembled in Figure 8) is oriented by the direction of an applied magnetic field and is pulled by the gradients in that field. The goal of this project is minimally invasive intraocular diagnosis and therapy. It has also been shown that the strong magnetic field inside an MRI can be used for wireless propulsion of soft-magnetic bodies in the bloodstream [30].

Crawling microrobots require more complicated propulsion mechanisms than those for swimming, but it is difficult to fabricate and power microscale actuators needed for crawling. One proposed solution is to grow muscle cells directly on the microrobot [31]. Muscle cells can extract biochemical energy from their environment, making them not only powerful, but also a promising autonomous actuation method.

Flying microrobots are probably the most challenging of any type of microrobot. They will be larger in size than other types of microrobots (even the smallest flying insects are significantly larger than microorganisms or the smallest crawling creatures), which simplifies fabrication. However, the level of autonomy needed in flying microrobots is enormous, and the control problems are difficult. The Micromechanical Flying Insect (MFI) Project is the most successful attempt at the design and construction of flying microrobots to date (Figure 15 and [32]). MFI prototypes use design and fabrication techniques that are scalable to smaller size if desired. Flying microrobots such as the MFI could be used for reconnaissance or search and rescue.

So far, each of the designs that we have considered involve a single microrobot agent. However, as size decreases to the sub-millimeter scale, it might be more promising to build a complex microrobot in a modular way, where the microrobot is composed of several different micromodules, each having a specific simple task. Consequently, a complex system behavior can be obtained by the integration of a large number of simple modules. For example, there can be modules providing power, generating locomotion, or performing sensing, manipulation, communication, or computation. The fabrication of these simple modules would be easier than the fabrication of a single complex agent. Modular robots also offer versatility in the navigation of unstructured environments.

To allow modularity, a robust mechanical connection is indispensable. However, scaling down existing connection designs from macroscale modular robots is unlikely to be successful, due to their complexity. Although no true modular microrobots have been demonstrated thus far, multiple research projects aim at them by using scalable technology in their prototypes. For example, in [33], shape-memory-alloy-based actuators are employed instead of motors, and modules as small as 2 cm^3 weighing 15 g (without the control unit) are demonstrated.

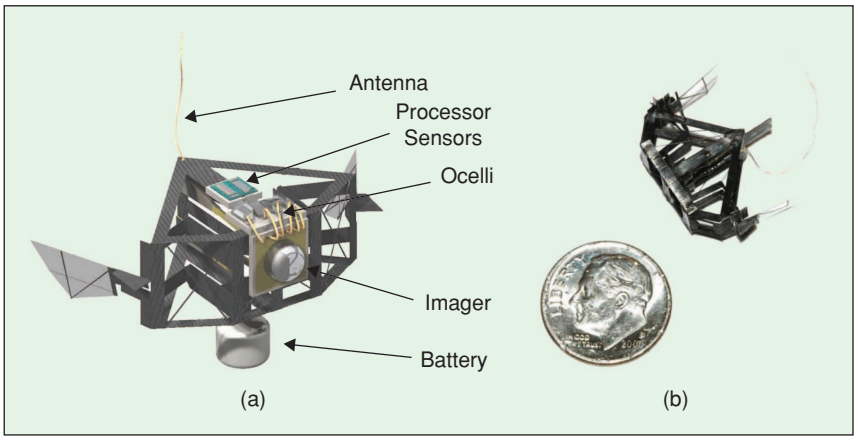

Figure 15. *(a) Artist's conception and (b) current prototype of the micromechanical flying insect. Images courtesy Ronald S. Fearing and Robert J. Wood, University of California, Berkeley, USA.*

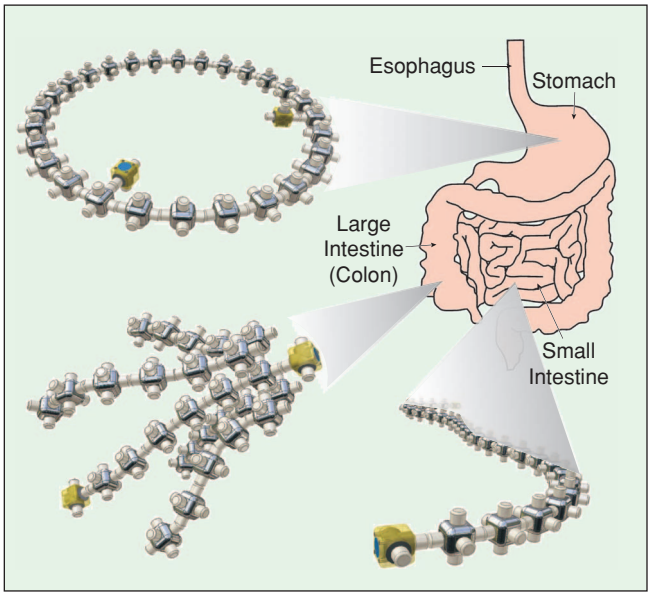

Figure 16. *Artist's conception of the ARES modular microrobotic system in various configuration in the GI tract. ARES images courtesy Paolo Corradi, Scuola Superiore Sant'Anna, Italy.*

One possible application area of modular microrobots is in biomedical applications, such as inside the human body. The goal of the Assembling Reconfigurable Endoluminal Surgical (ARES) system project [34] is to create a modular microrobot that is swallowed in parts and then assembled in the GI tract (Figure 16). Once assembled, it would be able to perform specific diagnostic and microsurgical tasks.

Harnessing Nature

Before the invention of trains and automobiles, mankind used animals to power simple machines. Similarly, as an alternative or supplement to man-made microrobots, we can harness biological organisms to work for us. These creatures already possess sensing ability, energetic autonomy, and intelligence that is well beyond the state of the art in engineering. Through a synthesis of biology, microfabrication, and robotics, amazing systems may be just around the corner. However, the control of live animals may raise some ethical questions.

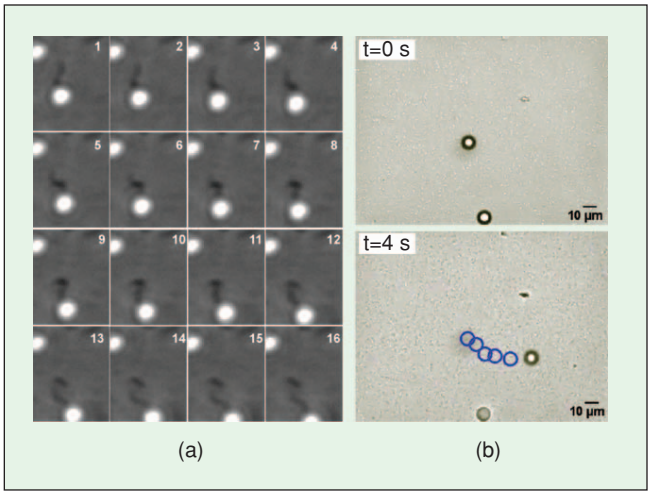

Figure 17. *(a) A 3-μm bead pushed by a single MTB, with direction controlled by magnetic field. Image courtesy Sylvain Martel, École Polytechnique de Montréal, Canada. (b) Two 10-μm beads, with several* S. marcescens *bacteria attached to the top bead. Motion of the top bead is shown with rings. Image courtesy Metin Sitti, Carnegie Mellon University, USA.*

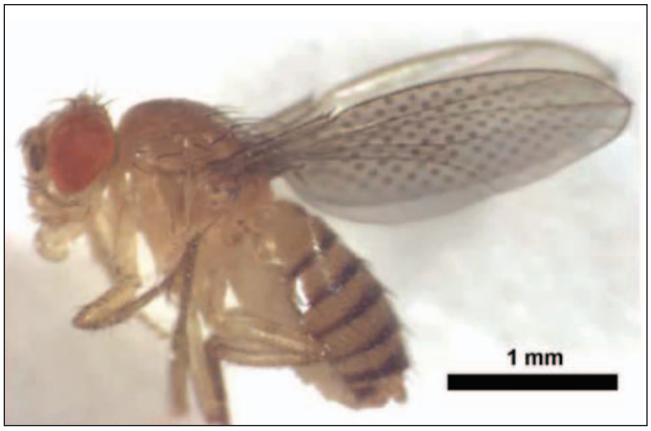

Figure 18. *Live Drosophila after thermal evaporation carrying a pattern of 100-nm-thick, 50-μm-wide indium circles. Image courtesy Babak A. Parviz and Angela J. Shum, University of Washington, USA.*

In [35], MC-1 magnetotactic bacteria (MTB), bacteria that contain internal compasses that result in them swimming persistently in one direction along a magnetic field, are attached to a bead, resulting in direction control of the bead through externally applied fields [Figure 17(a)]. The authors propose that such a bacterial-actuation scheme could be used to supplement their MRI-gradient scheme discussed previously [30], and could be used for targeted drug delivery in the human body. In [36], S. marcescens bacteria are attached to a bead, and their bacterial flagella are turned on and off by introducing various chemicals into their environment [Figure 17(b)]. Combining the results of [35] and [36] would result in fully actuated microorganisms.

In [37], the wings of live fruit flies (Drosophila) are used as a substrate for thermal evaporation of indium (Figure 18). The fruit flies are able to withstand the vacuum environment needed for microfabrication with a significant rate of survival. This research paves the way for the incorporation of MEMS technology on live organisms. By combining genetic engineering with MEMS-modified insects like those in [37], we could create hybrid biological flying microrobots that act as swarms of intelligent sensors.

On to Nanorobotics

This article provided an overview of the field of microrobotics, including the distinct but related topics of micromanipulation and microrobots. While many interesting results have been shown to date, the greatest results in this field are yet to come. Part II of this tutorial will present the nascent field of nanorobotics. We will find that the scaling of physical effects from the micro- to the nano-world is as drastic and as interesting as is the scaling from macro to micro.

Acknowledgments

The authors would like to thank Martin Probst for creating Figures 6 and 8, Mathias Moser and Chauncey Graetzel for creating Figure 12, Dominik Bell for creating Figure 13(b), and Karl Vollmers for creating Figure 14.

Keywords

Microrobot, micromanipulation, scaling, biomimetic, microfabrication, MEMS.

References

[1] R. Hooke, *Micrographia: Or, Some Physiological Descriptions of Minute Bodies Made by Magnifying Glasses*. London: J. Martyn and J. Allestry, 1665.

[2] E.M. Purcell, "Life at low Reynolds number," *Amer. J. Phys.*, vol. 45, no. 1, pp. 3–11, 1977.

[3] W.S.N. Trimmer, "Microrobots and micromechanical systems," *Sens. Actuators*, vol. 19, no. 3, pp. 267–287, 1989.

[4] F. Arai, D. Ando, T. Fukuda, Y. Nonoda, and T. Oota, "Micro manipulation based on micro physics: Strategy based on attractive force

reduction and stress measurement," in *Proc. IEEE/RSJ Int. Conf. Intelligent Robots Systems*, 1995, pp. 236–241.
[5] M. Wautelet, "Scaling laws in the macro-, micro- and nanoworlds," *Eur. J. Phys.*, vol. 22, no. 6, pp. 601–611, 2001.
[6] O. Cugat, J. Delamare, and G. Reyne, "Magnetic micro-actuators and systems (MAGMAS)," *IEEE Trans. Magn.*, vol. 39, no. 5, pp. 3607–3612, 2003.
[7] M.J. Madou, *Fundamentals of Microfabrication*, 2nd ed. Boca Raton, FL: CRC, 2002.
[8] J. Agnus, P. Nectoux, and N. Chaillet, "Overview of microgrippers and design of a micromanipulation station based on a MMOC microgripper," in *Proc. IEEE Int. Symp.Computational Intelligence Robotics Automation*, 2005, pp. 117–123.
[9] F. Beyeler, A. Neild, S. Oberti, D.J. Bell, Y. Sun, J. Dual, and B.J. Nelson, "Monolithically fabricated microgripper with integrated force sensor for manipulating microobjects and biological cells aligned in an ultrasonic field," *J. Microelectromech. Syst.*, vol. 7, no. 15, 2007.
[10] R.S. Fearing, "Survey of sticking effects for micro parts handling," in *Proc. IEEE/RSJ Int. Conf. Intelligent Robots Systems*, 1995, pp. 212–217.
[11] S. Fahlbusch and S. Fatikow, "Force sensing in microrobotic systems—An overview," in *Proc. IEEE Int. Conf. Electronics, Circuits Systems*, 1998, pp. 259–262.
[12] Y. Sun, B.J. Nelson, D.P. Potasek, and E. Enikov, "A bulk microfabricated multi-axis capacitive cellular force sensor using transverse comb drives," *J. Micromechanics Microeng.*, vol. 12, no. 6, pp. 832–840, 2002.
[13] N. Chronis and L.P. Lee, "Electrothermally activated SU-8 microgripper for single cell manipulation in solution," *J. Microelectromech. Syst.*, vol. 14, no. 4, pp. 857–863, 2005.
[14] Y. Sun, B.J. Nelson, and M.A. Greminger, "Investigating protein structure change in the zona pellucida with a microrobotic system," *Int. J. Robotics Res.*, vol. 24, no. 2–3, pp. 211–218, 2005.
[15] M.A. Greminger and B.J. Nelson, "Vision-based force measurement," *IEEE Trans. Pattern Anal. Machine Intell.*, vol. 26, no. 3, pp. 290–298, 2004.
[16] K.F. Böhringer, R.S. Fearing, and K.Y. Goldberg, "Microassembly," in *Handbook of Industrial Robotics*, S. Y. Nof, Ed., 2nd ed. New York: Wiley, 1999.
[17] G. Yang, J.A. Gaines, and B.J. Nelson, "Optomechatronic design of microassembly systems for manufacturing hybrid microsystems," *IEEE Trans. Ind. Electron.*, vol. 52, no. 4, pp. 1013–1023, 2005.
[18] S. Vogel, *Comparative Biomechanics: Life's Physical World*. Princeton, NJ: Princeton Univ. Press, 2003.
[19] A.B. Kesel, A. Martin, and T. Seidl, "Getting a grip on spider attachment: An AFM approach to microstructure adhesion in arthropods," *Smart Mat. Struc.*, vol. 13, no. 3, pp. 512–518, 2004.
[20] W. Federle and T. Endlein, "Locomotion and adhesion: Dynamic control of adhesive surface contact in ants," *Arthropod Struc. Develop.*, vol. 33, no. 1, pp. 67–75, 2004.
[21] Y. Sun, S.N. Fry, D.P. Potasek, D.J. Bell, and B.J. Nelson, "Characterizing fruit fly flight behavior using a microforce sensor with a new comb-drive configuration," *J. Microelectromech. Syst.*, vol. 14, no. 1, pp. 4–11, 2005.
[22] S.A. Jacobson and A.H. Epstein, "An informal survey of Power MEMS," in *Proc. Int. Symp. Micro-Mechanical Engineering*, 2003, pp. 513-520.
[23] N. Mano and A. Heller, "A miniature membraneless biofuel cell operating at 0.36 V under physiological conditions," *J. Electrochem. Soc.*, vol. 150, no. 8, pp. A1136–A1138, 2003.
[24] The Given Imaging PillCam Capsule Endoscopy. (2007) [Online]. Available: http://www.givenimaging.com/
[25] T. Honda, K.I. Arai, and K. Ishiyama, "Micro swimming mechanisms propelled by external magnetic fields," *IEEE Trans. Magn.*, vol. 32, no. 5, pp. 5085-5087, 1996.
[26] R. Dreyfus, J. Baudry, M.L. Roper, M. Fermigier, H.A. Stone, and J. Bibette, "Microscopic artificial swimmers," *Nature*, vol. 437, no. 6, pp. 862–865, 2005.
[27] D.J. Bell, S. Leutenegger, L.X. Dong, and B.J. Nelson, "Flagella-like propulsion for microrobots using a magnetic nanocoil and rotating electromagnetic field," in *Proc. IEEE Int. Conf. Robotics Automation*, 2007, pp. 1128-1133.
[28] K. Ishiyama, K.I. Arai, M. Sendoh, and A. Yamazaki, "Spiral-type micro-machine for medical applications," *J. Micromech.*, vol. 2, no. 1, pp. 77–86, 2003.
[29] K.B. Yesin, K. Vollmers, and B.J. Nelson, "Modeling and control of untethered biomicrorobots in a fluidic environment using electromagnetic fields," *Int. J. Robot. Res.*, vol. 25, no. 5–6, pp. 527–536, 2006.
[30] J.-B. Mathieu, G. Beaudoin, and S. Martel, "Method of propulsion of a ferromagnetic core in the cardiovascular system through magnetic gradients generated by an MRI system," *IEEE Trans. Biomed.Eng.*, vol. 53, no. 2, pp. 292–299, 2006.
[31] J. Xi, J.J. Schmidt, and C.D. Montemagno, "Self-assembled microdevices driven by muscle," *Nature Mat.*, vol. 4, no. 2, pp. 180–184, 2005.
[32] Micromechanical Flying Insect (MFI) Project. (2007) [Online]. Available: http://robotics.eecs.berkeley.edu/ronf/MFI/index.html
[33] E. Yoshida, S. Murata, S. Kokaji, A. Kamimura, K. Tomita, and H. Kurokawa, "Get back in shape! SMA self-reconfigurable microrobots," *IEEE Robot. Automat. Mag.*, vol. 9, no. 4, pp. 54–60, 2002.
[34] ARES Project. (2007) [Online]. Available: http://www.ares-nest.org/
[35] S. Martel, "Towards MRI-controlled ferromagnetic and MC-1 magnetotactic bacterial carriers for targeted therapies in arteriolocapillar networks stimulated by tumoral angiogenesis," in *Proc. IEEE Int. Conf. Engineering Medicine Biology Society*, 2006, pp. 3399-3402.
[36] B. Behkem and M. Sitti, "Bacterial flagella-based propulsion and on/off motion control of microscale objects," *Appl. Phys. Lett.*, vol. 90, no. 2, pp. 023 902(1–3), 2007.
[37] A.J. Shum and B.A. Parviz, "Vacuum microfabrication on live fruit fly," in *Proc. IEEE Int. Conf. Micro Electro Mechanical Systems*, 2007, pp. 179–182.

Jake J. Abbott received his Ph.D. in Mechanical Engineering at Johns Hopkins University in 2005. He is a postdoctoral research associate at the Institute of Robotics and Intelligent Systems at ETH Zurich, where he is developing biomicrorobots.

Zoltán Nagy received his M.S. in Mechanical Engineering at ETH Zurich in 2006. He is a Ph.D. candidate at the Institute of Robotics and Intelligent Systems at ETH Zurich, where he is developing biomicrorobots.

Felix Beyeler received his M.S. in Mechanical Engineering at ETH Zurich in 2004. He is a Ph.D. candidate at the Institute of Robotics and Intelligent Systems at ETH Zurich, where he is developing MEMS sensors and actuators.

Bradley J. Nelson received his Ph.D. in Robotics at Carnegie Mellon University in 1995. He became Assistant Professor at the University of Illinois at Chicago in 1995, Associate Professor at the University of Minnesota in 1998, and Professor of Robotics and Intelligent Systems at ETH Zurich in 2002. He is the head of the Multi-Scale Robotics Lab at the Institute of Robotics and Intelligent Systems at ETH Zurich, where his research involves microrobotics and nanorobotics.

Address for Correspondence: Bradley J. Nelson, Institute of Robotics and Intelligent Systems, ETH Zurich, ETH Zentrum, CLA H17.2, 8092 Zurich, Switzerland. E-mail: bnelson@ethz.ch.